

Weak localization and conductance fluctuations-like effects in Qubits driven by biharmonic signals

This content has been downloaded from IOPscience. Please scroll down to see the full text.

2014 J. Phys.: Conf. Ser. 568 052028

(<http://iopscience.iop.org/1742-6596/568/5/052028>)

View [the table of contents for this issue](#), or go to the [journal homepage](#) for more

Download details:

IP Address: 200.0.233.52

This content was downloaded on 05/02/2015 at 14:00

Please note that [terms and conditions apply](#).

Weak localization and conductance fluctuations-like effects in Qubits driven by biharmonic signals

Alejandro Ferrón^{1,2} Daniel Domínguez³ and María José Sánchez³

¹Instituto de Modelado e Innovación Tecnológica (CONICET-UNNE), 3400 Corrientes

²International Iberian Nanotechnology Laboratory (INL), Av. Mestre Jos Veiga, 4715-330, Braga, Portugal.

³Centro Atómico Bariloche and Instituto Balseiro, 8400 San Carlos de Bariloche, Argentina.

Abstract.

We investigate the effect of broken time reversal symmetry in flux qubits driven by a biharmonic magnetic flux signal with a phase lag. In the regime of large relaxation times, we explicitly compute the transition rate between the ground and the excited state, accounting for decoherence as a classical noise. Through a direct analogy between interference effects at the avoided level crossing and scattering events in weakly disordered electronic mesoscopic systems, the transition rate plays the role of an effective transmittance while the phase lag acts as a time reversal control parameter. Clear signatures of both weak localization and conductance fluctuations-like effects are predicted. Their behavior is studied as a function of the coherence rate, and a comparison with recent experimental results is performed. Our study shows that it is decoherence, and not the driving protocol, what limits the experimental detection of weak localization effects.

1. Introduction

Flux qubits (FQ) can be considered as artificial atoms whose energy levels are sensitive to an external magnetic flux. [1, 2] Its energy spectrum exhibits, as a function of the static magnetic flux, a rich structure of avoided crossings that can be explored by driving the FQ with a strong ac magnetic flux. This driving protocol -known as amplitude spectroscopy (AS) [3]- was successfully applied to reconstruct the FQ energy level spectrum [4, 5] and to estimate the qubit coherence times. [6] In the AS, the FQ is prepared in the ground state for a given value of the dc flux, and evolves quasi adiabatically under the driving, until at the first avoided crossing the state undergoes a transition and splits into a coherent superposition of transmitted and reflected amplitudes. In this way, each avoided crossing acts as an effective beam splitter in where a scattering event takes place. This analogy has been discussed in extent for FQ under weak driving, when the lowest two energy levels are explored and a single avoided crossing is attained by the amplitude of the ac flux.[3, 7]

Besides flux qubits, AS has been also employed in other systems, like charge qubits [12], ultracold molecular gases [13] and single electron spins. [14]

In addition, other phenomena relevant to quantum control- like population inversion- [15] have been tested with AS taking into account the coupling of the driven system to an environmental bath. [16]

One of the most efficient ways to probe coherent effects is by the phase sensitivity of the wave function to an external parameter that breaks time reversal symmetry. [18] In this way,



fundamental effects like weak localization (WL) and universal conductance fluctuations (UCF) have been tested in a wide variety of electronic mesoscopic system for decades. [19, 20, 21] UCF describe the sample specific fluctuations of the quantum conductance due to the sensitivity of the scattering configuration to a change in a parameter, like an external magnetic field or the electron density.[19] The WL effect originates from the constructive interference of pairs of time-reversed trajectories that survives disorder average. The enhanced return probability results in a negative quantum correction to the classical conductance, characterized by a peak in the resistance (dip in the conductance) at zero magnetic field. To suppress the WL effect, a critical magnetic field $B_c \sim 1/(D\tau_\phi)$ -being D the diffusion coefficient and τ_ϕ the dephasing time- is required. This critical field washes out the constructive interference and thus the weak localization correction. [20]

While a priori there is not an obvious connection between driven two level systems (TLS) and the physics of disordered electronic systems, the analogy between transitions at the avoided crossing and scattering events, suggests a way to study fluctuation effects in FQ. Along this line Gustavsson and collaborators [7] investigated, using as a test system the lowest two levels of a FQ driven by a biharmonic ac flux, fluctuations in the transition rate W , similar to UCF. The driving was implemented by a biharmonic signal $f(t) = A_1 \cos(\omega t + \alpha) - A_2 \cos(2\omega t)$ of fundamental frequency $\omega = 2\pi/T$, that could be turned asymmetric in time by means of a phase lag α . In addition, as the driving period $T \sim 8$ ns was comparable to the qubit dephasing time $T_2 = 1/\Gamma_2 \sim 10$ ns, coherence was preserved within one period, although multiphoton resonances were not clearly resolved because the resonance width was comparable to the resonances spacing.[9] In the experiments of Ref.[7] the energy relaxation time $T_1 = 1/\Gamma_1 \sim 20\mu s$ was much longer than the driving period T . Under this regime population could build up in the excited state as a function of time, decaying exponentially to the stationary state with a characteristic rate Γ , which was estimated from experimental results by a fitting procedure.[7] Although the restriction to the lowest two levels in the FQ constrains the mesoscopic analogy to the few-scatterers limit, the scattering events could be modified by either tuning the external dc flux or by changing the phase lag parameter α . In this way, the qubit could be driving up to four times through a given avoided crossing in one period T , given rise to non trivial interference patterns (see Fig. 1 (a)).

In this work we will show that, besides the detection of fluctuations analogous to UCF [7], weak localization (WL) effects could also be experimentally observable for the biharmonic driving protocol, in the regime of large coherence times, $T_2 \gg T$.

2. FQ under biharmonic driving

2.1. Transition rate and decoherence effects

In this section we derive an explicit expression for the decay rate W for a TLS under biharmonic driving in the presence of decoherence sources. The analysis is restricted to the lowest two levels of the FQ, and disregards additional energy levels not explored in the experiment of Ref.[7]. We start by writing the two level hamiltonian H for a FQ subjected to a biharmonic driving in the flux. In the TLS the diabatic states carry a persistent current $\mp I_p$ and are coupled via the tunneling matrix element Δ . [3, 4, 9] The detuning from the avoided crossing is defined as $\epsilon = 2I_p f$, with f the flux difference respect to half the superconducting flux quantum. [9] Under the biharmonic driving we define $\epsilon(t) = \epsilon + A_1 \cos(\omega t + \alpha) - A_2 \cos(2\omega t)$.

Figure 1 sketches the energy level diagram of the TLS and the biharmonic drive waveform chosen to traverse the avoided crossing four times in one period T . To account for decoherence we follow the approach of Berns *et. al.* [9] and include classical diagonal noise, neglecting energy relaxation processes (consistent with the experimental regime $T \lesssim T_2 \ll T_1$). For $\hbar = 1$, the

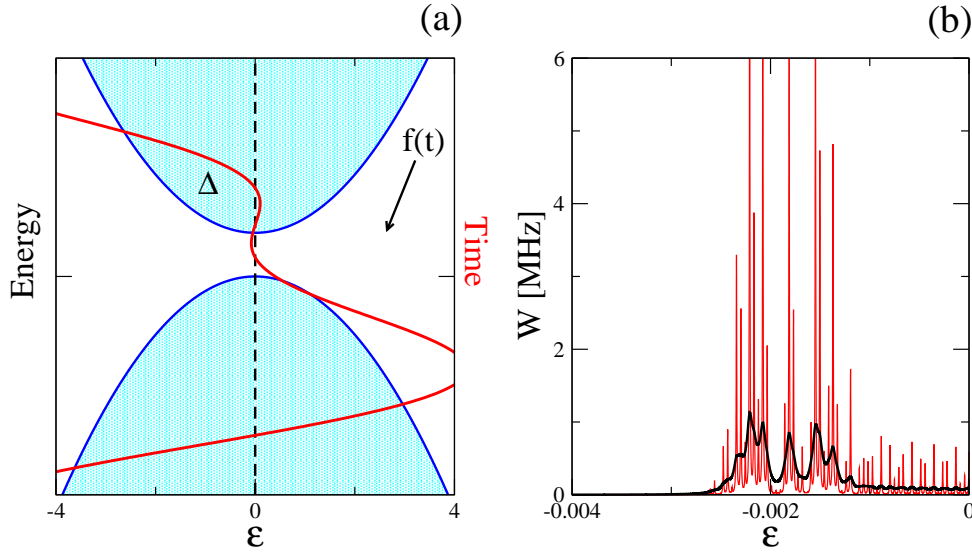


Figure 1. (color online) (a) Qubit energy diagram and biharmonic pulse for $\alpha = 0.4$ (b) Simulated transition rates W using modified Eq.(4) for qubit parameters $\Delta/h = 19 \text{ MHz}$, $\omega/(2\pi) = 125 \text{ MHz}$, $A_1 = 3 m\Phi_0$, $A_2 = 1.65 m\Phi_0$ and $\alpha = 0$ for $\Gamma_2 = 200 \text{ MHz}$ (black line) and $\Gamma_2 = 20 \text{ MHz}$ (red line).

hamiltonian H reads

$$H = -\frac{h(t)}{2}\hat{\sigma}_z - \frac{\Delta}{2}\hat{\sigma}_x$$

where $h(t) = \varepsilon(t) + \delta\varepsilon$ takes into account a classical fluctuating noise $\delta\varepsilon$ in the flux, and $\hat{\sigma}_z, \hat{\sigma}_x$ are Pauli matrices. After an unitary transformation, the hamiltonian can be written as

$$\tilde{H} = -\frac{1}{2} \begin{pmatrix} 0 & \Delta \\ \Delta^* & 0 \end{pmatrix},$$

where $\Delta(t) = \Delta e^{-i\phi(t)}$, and $\phi(t) = \int_0^t h(\tau)d\tau$. In the fast driving regime, where the driving frequency $\omega > \Delta$, the qubit population changes slowly on the time scale of T_2 . In this way the time evolution operator can be expanded as

$$U(t, t_0) = 1 - i \int_{t_0}^t \tilde{H}(\tau)d\tau + \mathcal{O}(\Delta^2),$$

and the transition rate W between the ground and the excited state can be computed using perturbation theory,

$$W = \lim_{\delta t \rightarrow \infty} \frac{|A_{t,t'}|^2}{\delta t}, \quad A_{t,t'} = \frac{1}{2} \int_{t'}^t \Delta(\tau)d\tau. \quad (1)$$

In order to evaluate W we must solve

$$W = \frac{1}{4} \int_{t'}^t \int_{t'}^t \Delta(\tau_1)\Delta^*(\tau_2)d\tau_1d\tau_2. \quad (2)$$

We expand the oscillating exponentials in Bessel functions and average $\delta\phi(t) = \int_0^t \delta\varepsilon(\tau)d\tau$ for a white noise model $\langle e^{i\delta\phi(t)} e^{-i\delta\phi(t')} \rangle = e^{-\Gamma_2|t-t'|}$. In this way, we get after integration of Eq.(1)

$$W = \frac{\Delta^2}{2} \sum_{nm'mm'} J_n(x_1)J_{n'}(x_1)J_m(x_2)J_{m'}(x_2) \quad (3)$$

$$e^{i(n-n')\alpha} e^{i\omega(n-n')t} e^{2i\omega(m-m')t} \frac{\Gamma_2}{(\varepsilon - n\omega - 2m\omega)^2 + \Gamma_2^2},$$

where we define $x_1 = A_1/\omega$ and $x_2 = -A_2/(2\omega)$. In the secular approximation, we neglect the fast oscillating terms, keeping only the $\omega(n - n') + 2\omega(m - m') \approx 0$ terms, obtaining

$$W = \frac{\Delta^2}{2} \Gamma_2 \sum_{nn'mm'} \lambda_{nn'mm'} \frac{\cos((n - n')\alpha)}{(\varepsilon - n\omega - 2m\omega)^2 + \Gamma_2^2}, \quad (4)$$

where $\lambda_{nn'mm'} = J_n(x_1)J_{n'}(x_1)J_m(x_2)J_{m'}(x_2)\delta_{n-n', 2(m-m')}$. The last equation shows the explicit dependence of the transition rate W on the phase lag α . In addition, as will be shown in the next section, W will display strong fluctuations both with α and the dc flux detuning ε .

2.2. Transition and decay rates. Computing fluctuations

In the scattering approach the transition rate W is identified with an effective transmission amplitude -the essential ingredient to compute the electronic conductance within the Landauer formalism. [11] In addition, to complete the analogy with electronic transport in disordered mesoscopic systems, the parameter α plays the role of an effective magnetic (flux) field. In Ref.[7], the experimentally accessible quantity is the decay rate Γ . From phenomenological rate equations that describe the TLS dynamics, it is straightforward to show that $\Gamma = 2W + 2\Gamma_1$. [9] For large relaxation times T_1 , it is satisfied that $\Gamma_1 \ll W$ and then $W \approx \Gamma/2$. Larger values of Γ_1 would require the explicit inclusion of relaxation processes in the analysis to avoid important differences between W and the experimentally measured Γ . [22] In the following we will keep our analysis consistent with the hypothesis $W \approx \Gamma/2$ and in this way, Eq.(4) provides an explicit expression to compute Γ . In Ref. [7], the specific value of the amplitudes ratio $A_2/A_1 = 0.55$ has been selected. In this way, the FQ has been driven up to four times through the avoided crossing in one period T , giving three different interference phases (one phase for two successive passages) and eight possible superposition states.

Figure 1 (b) shows the value of W obtained from Eq.(4) for the qubit parameters used in Ref.[7], i.e. $\Delta/h = 19 \text{ MHz}$, $\omega/(2\pi) = 125 \text{ MHz}$, $A_1 = 3m\Phi_0$ and $A_2 = 1.65m\Phi_0$ ($A_2/A_1 = 0.55$). The experimentally reported values of $T_{2exp} = 10 - 20 \text{ ns}$ give $\Gamma_{2exp} = 50 - 100 \text{ MHz}$. We explicitly set the phase lag $\alpha = 0$. W exhibits a clear pattern of oscillations as a function to the static flux detuning ε . These strong fluctuations are a manifestation of the sensitivity of the total phase accumulated during one period of the driving with the value of ε , as a consequence of the strong asymmetry in the driven signal. When analyzing the behavior of W as a function of the decoherence rate, we find that for small values of Γ_2 , the transition rate exhibits high and sharp peaks that turn smoother and wider as the decoherence rate is increased. This behavior is fully consistent with the transition from the non overlapping to the overlapping resonances limit, also observed experimentally for the single harmonic driving protocols. [3, 4] In Fig. 2 we plot W from Eq. (4) for the same parameters used in Fig 1 (b) but for $\alpha \neq 0$. We can appreciate the results for $\alpha = 0.2$ (left panel, Fig. 2 (a)) and $\alpha = 0.4$ (right panel, Fig. 2 (b)), in both cases the structure of the peaks described in Fig.1 (b) is also obtained. Indeed, the asymmetry of the peaks as a function of the detuning ε is clearly observed.

For the chosen amplitudes ratio and depending on ε the wave form may drive the qubit through the avoided crossing zero, two or four times per cycle, producing different phase accumulations and interference conditions. In addition, the total phase accumulated- besides its dependence on ε - strongly depends on the biharmonic waveform, which is controlled by the asymmetry parameter α . To explore these effects, in Fig 3 we construct a map of the transition rate W as a function of the detuning and the phase lag. W exhibits in its interference patterns strong fluctuations, both as function of ε and α , in fully agreement with the fluctuations detected

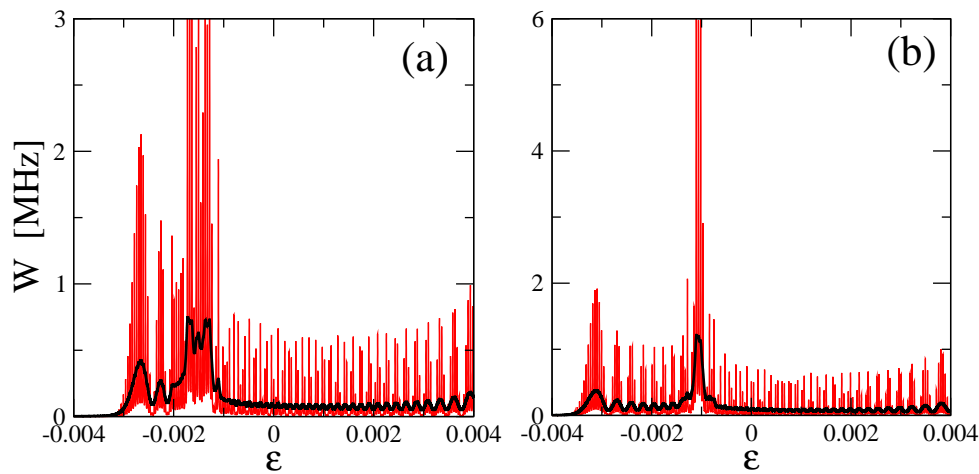


Figure 2. (color online) Simulated transition rates W using Eq.(4) for qubit parameters $\Delta/h = 19 \text{ MHz}$, $\omega/(2\pi) = 125 \text{ MHz}$, $A_1 = 3 m\Phi_0$ and $A_2 = 1.65 m\Phi_0$ for $\Gamma_2 = 200 \text{ MHz}$ (black line) and $\Gamma_2 = 20 \text{ MHz}$ (red line). (a) $\alpha = 0.2$ and (b) $\alpha = 0.4$.

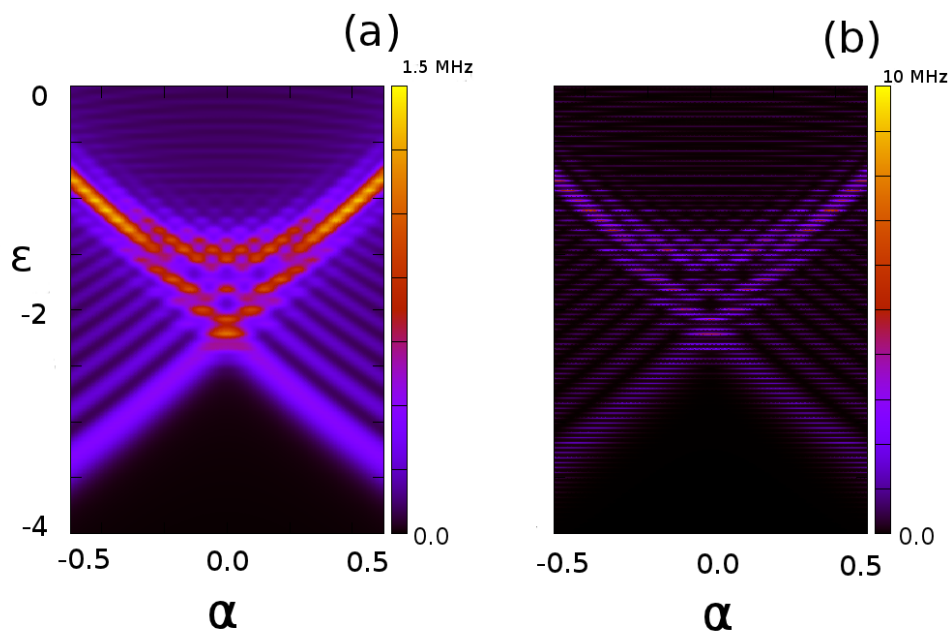


Figure 3. (color online) Contour plot of transition rate W using Eq.(4) for qubit parameters $\Delta/h = 19 \text{ MHz}$, $\omega/(2\pi) = 125 \text{ MHz}$, $A_1 = 3 m\Phi_0$ and $A_2 = 1.65 m\Phi_0$. (a) $\Gamma_2 = 200 \text{ MHz}$ and (b) $\Gamma_2 = 20 \text{ MHz}$.

experimentally in the FQ population interference patterns.[7] Another interesting feature is the strong effect of the decoherence rate on the results, as we already mentioned. We can appreciate important qualitative differences in the results for $\Gamma_2 = 200 \text{ MHz}$ (Fig. 3 (a)) and $\Gamma_2 = 20 \text{ MHz}$ (Fig. 3 (b)).

As we show below, even after averaging over different values of the dc flux, strong fluctuations

are still visible in W as a function of α . In order to evaluate them, we can compute the average $\langle W \rangle = \frac{1}{2\varepsilon^{max}} \int_{-\varepsilon^{max}}^{\varepsilon^{max}} W d\varepsilon$ and using Eq. (4) we can evaluate the integral, obtaining

$$\langle W \rangle = \frac{\Delta^2}{4\varepsilon^{max}} \sum_{nn'mm'} \lambda_{nn'mm'} \cos((n - n')\alpha) \left[\arctan\left(\frac{n\omega + 2m\omega + \varepsilon^{max}}{\Gamma_2}\right) - \arctan\left(\frac{n\omega + 2m\omega - \varepsilon^{max}}{\Gamma_2}\right) \right]. \quad (5)$$

In the same way we can compute

$$\langle W^2 \rangle = \frac{1}{2\varepsilon^{max}} \int_{-\varepsilon^{max}}^{\varepsilon^{max}} W^2 d\varepsilon. \quad (6)$$

Although $\langle W^2 \rangle$ does not have a simple analytic expression, its numerical calculation is straightforward. In Fig 4 we plot both the average transition rate $\langle W \rangle$ and its fluctuations $\sigma = \sqrt{\langle W^2 \rangle - \langle W \rangle^2}$ for the experimental FQ parameters but for different values of the decoherence rate Γ_2 . We can see that, for values of the decoherence rate similar to the experimental ones $\Gamma_2 \sim 20 - 200 MHz$, $\langle W \rangle$ is almost independent of α and σ - characterized as the UCF- presents a well defined peak at $\alpha = 0$, in full agreement with Ref.[7].

The fingerprint of the WL effect should be a dip in $\langle W \rangle$ at $\alpha = 0$ - a dip in the average transmission probability- following the electronic transport analogy. In the experiments of Ref.[7] this WL effect was not observed. However, there is not an experimental constrain in the driving protocol that precludes the observation of WL. As we show, it is the decoherence time T_2 which limits the width of the WL peak, and its experimental detection. From the theory of disordered electronic systems [20] the value of the critical magnetic field needed to destroy the WL peak is $B_c \sim 1/(D\tau_\phi)$, being D the diffusion coefficient and $\tau_\phi \propto T_2$. In the present analysis, the critical value α_c needed to destroy the WL correction, should scale as $\alpha_c \sim 1/(T_2)$. Thus it is expected, that large decoherence times should be needed in order to experimentally detect the whole WL peak with accessible values of α_c . Consistent with this analysis, in fig. 4 we show that for $\Gamma_2 = 6 MHz$ there is a well defined dip present in $\langle W \rangle$ at $\alpha = 0$. As a consequence, we can conclude that for long decoherence time ($T_2 \simeq 150 ns$) WL should emerge in the experiments.

3. Conclusions and perspectives

In this work we have tested fluctuation effects associated to broken time reversal symmetry in FQ driven by a biharmonic ac magnetic flux. Employing a simplified model that accounts only for decoherence, we computed the transition rate W which displays strong fluctuations as a function of the dc flux detuning and the time reversal parameter α . The results presented are derived under the assumptions that $W \ll \Gamma_2 = T_2^{-1}$ and $T \lesssim T_2 \ll T_1$, and in agreement with the experimentally reported regime of Ref. [7]. However it is not difficult to attain experimental regimes in which some of the above conditions are not satisfied. In particular, for small driving frequencies or larger decoherence times, T_2 , important difference could emerge between the transition rate W , Eq.(4), and the measured decay rate Γ . Besides conductance fluctuations-like effects, we also show that WL effect could be detected for the biharmonic driving protocol. However to observe this effect, the experiments should be performed in a more coherent regime, in which larger values of T_2 could be attained. By increasing the driving amplitude, more avoided crossings of the FQ can be reached, enabling the computation of averages and fluctuations with reasonable accuracy. This regime is experimentally attainable as the amplitude spectroscopy experiments have been proven. In addition the extension of the calculations for a realistic model that includes, besides decoherence, relaxation processes due to the interaction of the FQ with the circuitry environment is also under study. [22]

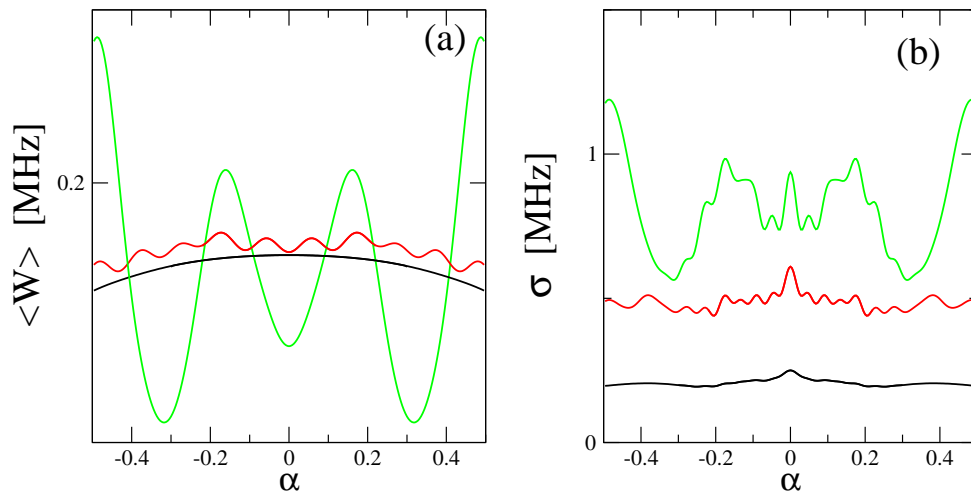


Figure 4. (color online) (a) Averaged transition rate $\langle W \rangle$ and (b) σ for qubit parameters $\Delta/h = 19$ MHz, $\omega/(2\pi) = 125$ MHz, $A_1 = 3 m\Phi_0$ and $A_2 = 1.65 m\Phi_0$ calculated using Eq.(4), (5) and (6) for $\Gamma_2 = 200$ MHz (black line), $\Gamma_2 = 20$ MHz (red line) and $\Gamma_2 = 6$ MHz (green line). The averages were performed in the range $-4m\Phi_0$ to $4m\Phi_0$.

Acknowledgments

We acknowledge support from CNEA, CONICET and ANPCyT PICT2011-1537.

References

- [1] Orlando T P *et al* 1999 *Phys. Rev. B* **60** 15398
- [2] Chiorescu I *et al* 2003 *Science* **299** 1869
- [3] Oliver W D *et al* 2005 *Science* **310** 1653
- [4] Berns D M *et al* 2008 *Nature* **455** 51; Oliver W D and Valenzuela S O 2009 *Quantum Inf. Process* **8** 261 (2009)
- [5] Ferrón A, Domínguez D and Sánchez M J 2010 *Phys. Rev. B* **82** 134522
- [6] Shevchenko S N, Ashhab S and Nori F 2010 *Phys. Rep.* **492** 1
- [7] Gustavsson S, Bylander J and Oliver W D 2013 *Phys. Rev. Lett.* **110** 016603
- [8] You J Q and Nori F 2011 *Nature* **474** 589
- [9] Berns D M *et al* 2006 *Phys. Rev. Lett.* **97** 150502
- [10] Izmailkov A *et al* 2008 *Phys. Rev. Lett.* **101** 017003
- [11] Datta S 1995 *Electronic transport in Mesoscopic Systems* (Cambridge: Cambridge University Press)
- [12] Nakamura Y, Pashkin Y A and Tsai J S 2001 *Phys. Rev. Lett.* **87** 246601; Sillanpaa M *et al* 2006 *Phys. Rev. Lett.* **96** 187002; Wilson CM *et al* 2007 *Phys. Rev. Lett.* **98** 257003
- [13] Mark M *et al* 2007 *Phys. Rev. Lett.* **99** 113201
- [14] Huang P *et al* 2011 *Phys. Rev. X* **1** 011003
- [15] Weber J 1959 *Rev. Mod. Phys.* **31** 681; Astafiev O *et al* 2007 *Nature* **449** 588; You J Q *et al* 2007 *Phys. Rev. B* **75** 104516
- [16] Ferrón A, Domínguez D and Sánchez M J 2012 *Phys. Rev. Lett.* **82**,134522
- [17] Ferrón A and Domínguez D 2010 *Phys. Rev. B* **81** 104505
- [18] For a review, see Althuler B L, Lee P A and Webb R A 1991 *Mesoscopic Phenomena in Solids* (Amsterdam: Elsevier)
- [19] Benoit A *et al.* 1986 *Phys. Rev. Lett.* **58** 2343; Washburn S and Webb R A 1992 *Rep. Prog. Phys.* **55** 1311 (1992)
- [20] Bergmann G 1982 *Phys. Rev. B* **25** 2937 (1982); Bishop D J *et al.* 1982 *Phys. Rev. B* **26** 773
- [21] Akkermans E, Montambaux C, Pichard J L and Zinn-Justin J 1994 *Mesoscopic quantum physics* (Amsterdam: Elsevier)
- [22] Ferrón A, Domínguez D and Sánchez M J 2014 in preparation